CHALMERS
UNIVERSITY OF TECHNOLOGY

Influence of Displaced Waveguide Feed on Terahertz Power Measurements

IEEE Journal of Microwaves

Received 9 October 2025; revised 3 December 2025; accepted 4 December 2025.

Digital Object Identifier 10.1109/JMW.2025.3641844

Influence of Displaced Waveguide Feed on Terahertz Power Measurements

JAN STAKE [1] (Fellow, IEEE), STEVEN DURANT [2], LUCY WILLIAMSON [2], AND JEFFREY HESLER [1,2] (Fellow, IEEE)

(Regular Paper)

[1]Department of Microtechnology and Nanoscience, Chalmers University of Technology, 412 96 Gothenburg, Sweden
[2]Virginia Diodes Inc. (VDI), Charlottesville, VA 22902 USA

CORRESPONDING AUTHOR: Jan Stake (email: jan.stake@chalmers.se).

ABSTRACT Calorimetric sensors that incorporate a rectangular waveguide interface facilitate absolute and precise power measurements. Moreover, by using a waveguide taper that transitions to a smaller, single-mode waveguide feed, the bandwidth limitation of a standard waveguide band can be extended to higher frequencies, enabling accurate power measurements across a wide portion of the electromagnetic spectrum. For aligned waveguide apertures without discontinuities, the incident field remains in the fundamental mode, thereby enabling broadband power measurements. In this work, we present a systematic study of intentionally misaligned waveguide junctions, specifically symmetrical *H*-plane or *E*-plane displacements at the WR-10 input flange of a PM5B power sensor, and their overall impact on the mismatch. The return loss was measured and simulated over a frequency span of 75 GHz to 1100 GHz, exceeding a decade. Electromagnetic simulations agree well with the experimental results, showing an excellent return loss for the aligned junction and a degradation attributed to the onset of higher-order parasitic modes in the misaligned case. In particular, it is found that the onset of a propagating TM_{11} mode due to *E*-plane displacement is the primary concern, while *H*-plane displacements have a negligible effect. However, a return loss better than 20 dB can be maintained if this offset is kept below 4% of the waveguide height. Hence, broadband, precise, and absolute power measurements are feasible provided that waveguide feed junctions are aligned and fabricated with high tolerances.

INDEX TERMS Calorimetry, electromagnetic propagation, metrology, millimeter wave measurements, power measurements, rectangular waveguides, sensors, submillimeter wave measurements, terahertz radiation, waveguide discontinuities.

I. INTRODUCTION

Absolute power measurements traceable to primary standards in the terahertz frequency region (100 GHz - 10 THz) [1] present many challenges due to high transmission loss, high noise levels, and difficulty in packaging a sensor [2]. There are numerous ways to convert terahertz radiation to a readable signal, typically based on a thermal or electronic mechanism; see the comprehensive review by Lewis [3]. The detection of the thermal expansion of a gas (e.g., Golay cell) or change in electrical resistance (bolometer) are common calorimetric[1] examples, while a Schottky barrier diode is a typical electronic example. The latter exhibits a fast response time and low Noise-Equivalent Power (NEP) level but is sensitive to signal frequency. On the other hand, a calorimeter is inherently insensitive to frequency and easy to calibrate using the same absorber with a known applied amount of power. Therefore, calorimeters based on electrical substitution radiometry are the standard choice for absolute power measurements across a vast part of the electromagnetic spectrum.

A waveguide-based power sensor is convenient for microwave and submillimeter wave measurements, providing a well-defined electrical interface and reference plane. Macpherson and Kerns introduced the first waveguide

[1]A historical note is that Herschel used a thermometer to observe infrared radiation, which he named "calorific" rays, in 1800 [4] by conducting an experiment initially proposed by Émilie du Châtelet around 1737 [5].

calorimeter in 1953 [6], and Vowinkel demonstrated a broadband calorimeter for precision measurement of millimeter- and submillimeter-wave power in 1980 [7]. Power measurements above the waveguide band, introducing propagation of higher-order modes, were shown to be accurate since the waveguide loads are broadband and relatively insensitive to higher-order modes. However, these first waveguide calorimeters suffered from a slow response time of tens of seconds. In 1999, Neal Erickson introduced a compact, fast, and sensitive power meter, operating from 75 GHz to the THz range [8]. The time constant was reduced to seconds with a feedback loop circuitry, and the sensor has a WR-10 test port with a well-matched waveguide termination. Later, the calorimetric power meter was further improved and became commercially available, known as the Erickson model PM1B [9], having sensitivity and stability sufficient to measure a power level well below 1 μW. Since then, it has become the de facto standard instrument for terahertz power measurements and, since 2009, continuously upgraded by Virginia Diodes to the current version VDI Erickson PM5B [10]. Recently, national metrology institutes (NMIs) have been able to perform traceable calibration of power measurements up to 170 GHz [11], [12], and Stokes et al. [13] reported a comprehensive evaluation of the PM5 sensor at W-band compared to a primary standard micro-calorimeter system. For higher frequencies, precise power measurements have been demonstrated in the 220-330 GHz range with a single-mode waveguide calorimeter [14]. However, realizing and packaging a single-mode waveguide sensor at shorter wavelengths becomes increasingly challenging. Alternatively, extending traceable power measurements to higher waveguide bands requires a better understanding of the multimode propagation and absorption in the waveguide feed and load, respectively. However, these high-order waveguide modes, which are excited due to discontinuities, are not necessarily a problem as long as they are well absorbed in the waveguide load and not reflected.

In this paper, we present measurements and simulations of the return loss of the PM5B power meter between 75 GHz and 1100 GHz for aligned and symmetrically displaced waveguide feeds in *E*- and *H*-planes, respectively. We show what parasitic propagating modes can be excited due to a misaligned waveguide junction, which can be observed in the frequency response of the return loss. However, this can be mitigated with the careful alignment of the waveguide feed with the sensor WR-10 test port, resulting in an excellent return loss across a wide frequency span from 75 GHz to 1100 GHz.

II. METHODS

The internal waveguide of the VDI Erickson PM5B power meter is a thin, Ni-alloy, WR-10 waveguide with a gold-plated interior to ensure sufficient thermal resistance, low heat capacity, and low signal attenuation. The incident principal TE_{10} field is guided to the power meter via a linear double waveguide taper [15] followed by a short straight WR-10 section, as shown in Fig. 1. The incoming signal is then absorbed in a load about 24 mm from the waveguide flange [9]. The load is designed to absorb the principal waveguide mode across a wide frequency range. However, most high-order parasitic modes are still efficiently absorbed, provided their E_x-field component is less significant. The different waveguide components are fabricated with high tolerances according to IEEE Std 1785.1-2 [16], [17], while the alignment to the flange of the power meter is less accurate. The influence of this aperture misalignment, a slight symmetrical *E*-plane or *H*-plane displaced waveguide feed, is the subject of this study. The measurement reference plane is located at the single-mode port of the waveguide taper; see Fig. 1.

A. E- AND H-PLANE DISPLACED WAVEGUIDE FEED

Uncertainties in waveguide cross-section dimensions and flange alignments will introduce systematic errors in scattering parameter measurements [18]. Therefore, reflections at a junction between two hollow waveguides have been extensively studied - largely covered in Marcuvitz's waveguide handbook from 1951 [19] and in an excellent report from 1989 by Bannister et al. [20]. For the single-mode case, Hunter [21] analyzed two identical waveguides with a transverse displacement normal to the broad wall (*E*-plane displacement) or the narrow wall (*H*-plane displacement), using a modal analysis technique [22]. The incident TE_{10} mode excites longitudinal-section electric modes (LSE, TM_{1p}/TE_{1p}), where p is an odd integer, to ensure $E_x = 0$, for the *E*-plane displacement, and the *H*-plane displacement involves high-order TE modes. Therefore, for the single-mode case, these symmetrical displacements can be represented with a shunt capacitance for the *E*-plane displacement and shunt inductance for the *H*-plane displacement, respectively [20]. In a junction between identical, displaced, overmoded guides, the incident TE_{10} field will also couple to propagating TM_{1p}/TE_{1p} modes for an *E*-plane displacement and TE_{m0} modes for an *H*-plane displacement, where p is an odd integer, $m \geq 1$ is an integer to fulfill the boundary condition for a symmetric displacement and assuming perfect electrical conductor walls. A finite wall conductivity will introduce a minor coupling to additional modes, including a TE_{01}-mode for *H*-plane displacement. Thus, noteworthy parasitic modes, $k_c^2 = (m\pi/a)^2 + (p\pi/b)^2$, that can be excited by an incoming TE_{10} field in a displaced WR10-waveguide feed are summarised in Table 1.

The waveguide junction between the sensor and the rectangular waveguide feed (Fig. 1) was displaced by using an alignment dowel with a diameter smaller than the holes to create a loose fit, similar to the method described by Li et al. [23]. A misalignment of approximately 0.08 mm was achievable and measured using a waveguide shim, as shown in the photograph in Fig. 2.

B. SIMULATIONS

Full electromagnetic simulations were conducted using a commercial frequency-domain solver (Ansys HFSS). The waveguide walls were assigned a finite conductive boundary (gold) with an electrical conductivity of $\sigma = 4.1 \times 10^7$ S/m. A finite element mesh was generated for a solution frequency

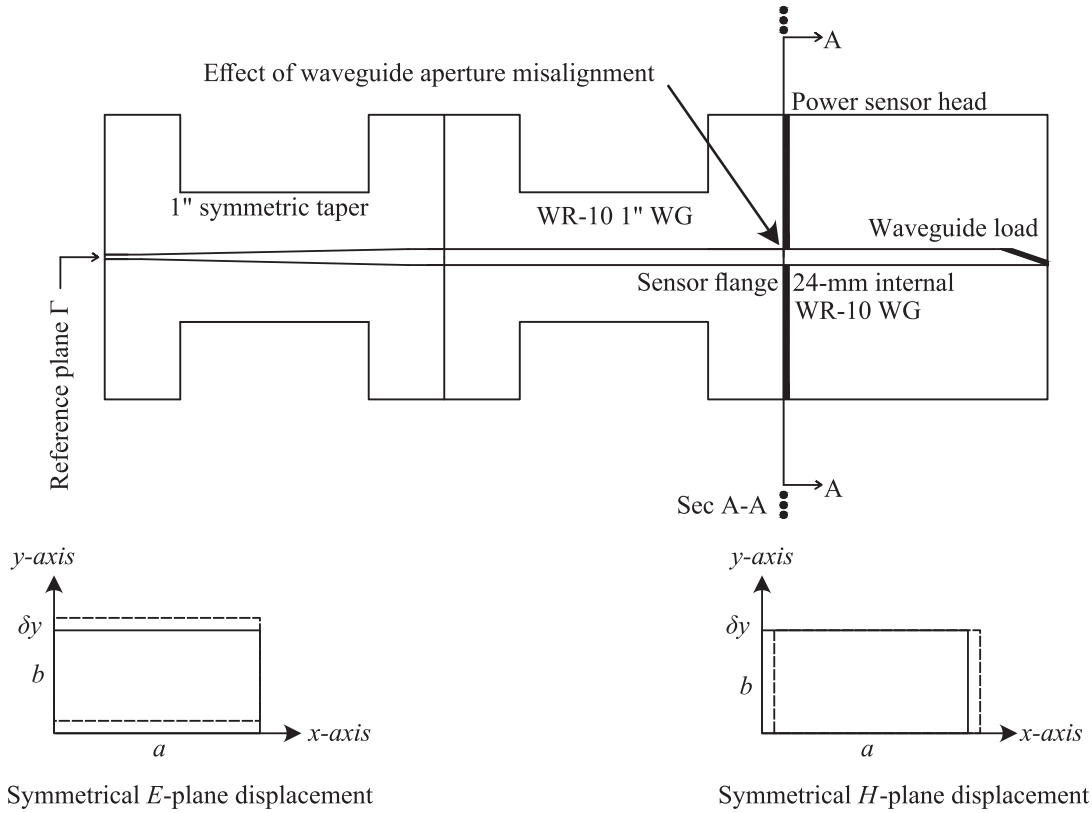

FIGURE 1. Illustration of the power meter with waveguide feed. In this study, the waveguide feed is displaced (δx, δy) relative to the internal waveguide of the power sensor to examine the influence of high-order modes. The reference plane for measurements of the reflection coefficient, Γ, is indicated. NB! The drawing is not to scale.

TABLE 1. Coupling to Parasitic Modes in Misaligned Waveguide (WR-10) Apertures

Waveguide mode	f_c (GHz)	Displaced waveguide
TE_{20}	118	*H*-plane
TE_{01}	118	*H*-plane
TM_{11}, TE_{11}	132	*E*-plane
TE_{40}	236	*H*-plane
TM_{13}, TE_{13}	359	*E*-plane
TM_{15}, TE_{15}	593	*E*-plane
TM_{17}, TE_{17}	828	*E*-plane
TM_{19}, TE_{19}	1064	*E*-plane

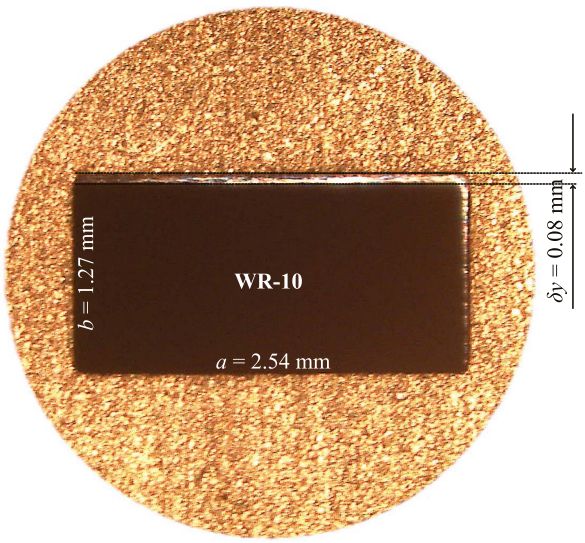

FIGURE 2. Waveguide misalignment. A microscope photograph showing a displaced waveguide aperture. The displacement was measured using a waveguide shim.

in the middle of each waveguide band and refined until the magnitude of the complex reflection coefficient, $|\Gamma|$, between two consecutive passes was less than 0.01. Symmetry is broken due to the displaced waveguides (δx, δy), and therefore, the entire structure must be solved, resulting in a large mesh and a challenging problem for higher frequency bands (see Fig. 3). However, for the aligned case ($\delta x = \delta y = 0$), *H*-plane symmetry was applied to reduce the size of the finite-element mesh. For each waveguide band (Table 2), only one mode can sustain and propagate at the waveguide feed port (taper), and the finite element mesh was solved at 101 frequency points and using second-order basis functions. The cross-section of the waveguide was assumed to

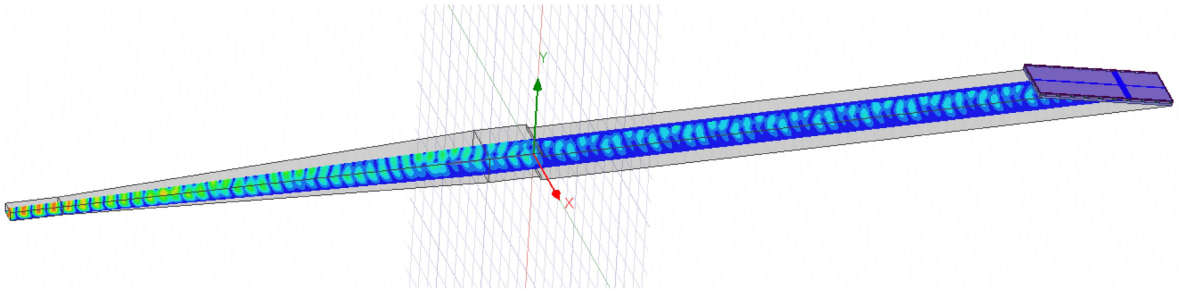

FIGURE 3. Electromagnetic model for the WR3.4 (220–330 GHz) waveguide band. Simulations of the electromagnetic field for an *E*-plane displaced waveguide feed with $\delta y = 0.2$ mm. The structure was excited using a single-mode (TE_{10}) wave port, shown on the left of the figure.

TABLE 2. Test Equipment for Reflection Coefficient Measurements of PM5B Power Sensor

Band Designation	Band (GHz)	Internal dimensions (mm × mm)	VNA frequency extender VDI model number	Waveguide taper 1-inch long
WM-2540 (WR-10)	75-110	2.540 × 1.270	WR10-VNAX-TxRx-M20	WR10SWG1R5
WM-1651 (WR-6.5)	110-170	1.651 × 0.826	WR6.5-VNAX-TxRx-M20	WR6.5-10TR3
WM-1295 (WR-5.1)	140-220	1.295 × 0.648	WR5.1-VNAX-TxRx-M20	WR5.1-10TR3
WM-864 (WR-3.4)	220-330	0.864 × 0.432	WR3.4-VNAX-TxRx-M20	WR3.4-10TR3
WM-570 (WR-2.2)	330-500	0.570 × 0.285	WR2.2-VNAX-TxRx-M20	WM570-10TR3
WM-380 (WR-1.5)	500-750	0.380 × 0.190	WR1.5-VNAX-TxRx-M20	WM380-10TR3
WM-250 (WR-1.0)	750-1100	0.250 × 0.125	WR1.0-VNAX-TxRx-M20	WM250-10TR3

RF waveguide name designation. WR-Rectangular waveguide, where the number represents the waveguide width in mils, multiplied by 10. 'W' stands for waveguide, 'M' for metric, and the number is the waveguide width in micrometers [16].

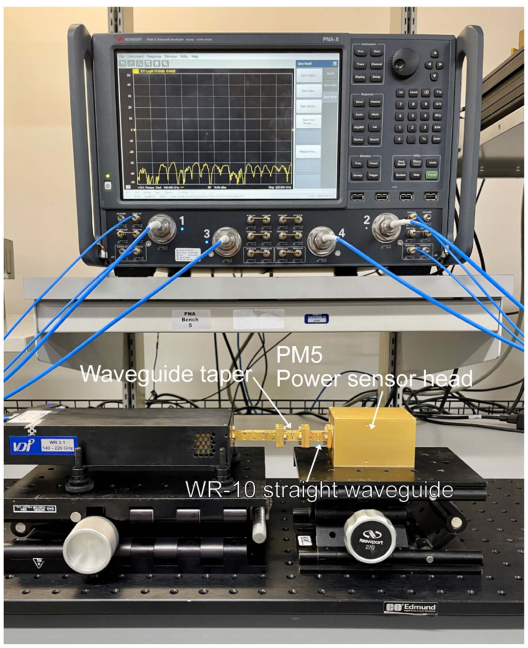

FIGURE 4. Measurement set-up. Photograph showing the reflection coefficient measurements of the PM5 power meter and a waveguide taper.

be perfectly rectangular, and the influence of rounded corners was neglected [24]. For simplicity, the 1-inch-long straight waveguide in Figs. 1 and 4 was excluded from simulations. The model was successfully solved across a frequency range of five octaves for the complete model and a decade for the aligned, symmetrical case.

C. MEASUREMENT SET-UP

The reflection coefficient, $\Gamma = S_{11}$, of the PM5B power meter (S/N 601V) was measured between 67 GHz and 1100 GHz using a vector network analyzer (Keysight N5222B) with VDI frequency extender modules, see Table 2 and Fig. 4. Prior to S-parameter calibration, the extender units were allowed to thermally stabilize for at least one hour. Then, a standard waveguide SOL calibration (short, quarter delay short, load) was carried out for each waveguide band, using 2001 frequency points and an IF bandwidth of 500 Hz. With the reference plane at the extender module waveguide port, the calibration was carefully evaluated by measuring a second load before the characterization of the PM5 power meter. For each band, a 1-inch-long waveguide taper to WR-10 was used, see Table 2, except for the WR-10 band, a straight 1-inch waveguide was used, all with a UG-387 waveguide flange [17].

III. RESULTS

For each waveguide band, between WR-10 and WM-250, the reflection coefficient was measured for a power sensor with an aligned (Fig. 5) and an *E*-plane displaced (Fig. 6) waveguide feed to the aperture of the sensor WR-10 test port. This data indicates that a careful alignment of the waveguide feed to the sensor WR-10 test port results in a return loss better than 25 dB across a wide frequency span from 75 GHz to

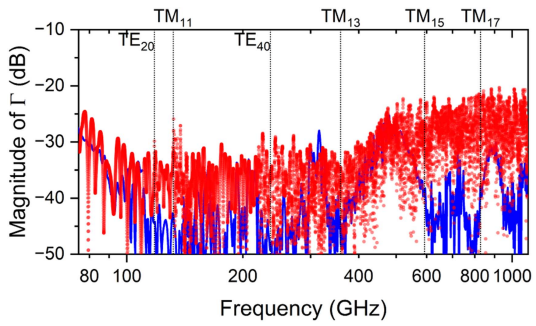

FIGURE 5. Reflection coefficient for an aligned waveguide feed. Measured (red) and simulated (blue) magnitude of reflection coefficient, $|\Gamma|$, versus frequency of the PM5B power meter with an aligned waveguide feed. Note: Data is combined for each waveguide band WR-10, WR-6.5, WR-5.1, WR-3.4, WR-2.2, WR-1.5, and WR-1.0.

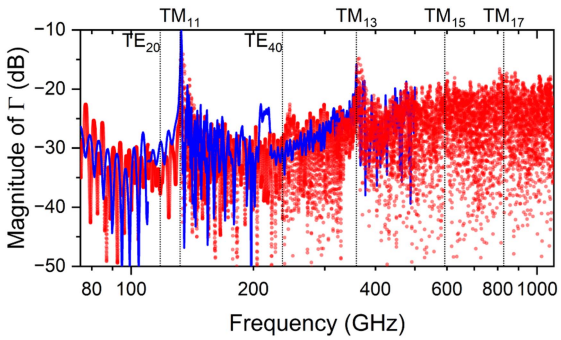

FIGURE 6. Reflection coefficient for an *E*-plane displacement. Measured (red) and simulated (blue) magnitude of reflection coefficient, $|\Gamma|$, versus frequency of the PM5B power meter with a symmetrically *E*-plane displaced waveguide feed of circa $\delta y = 0.08$ mm. Note: Data is combined for each waveguide band WR-10, WR-6.5, WR-5.1, WR-3.4, WR-2.2, WR-1.5, and WR-1.0.

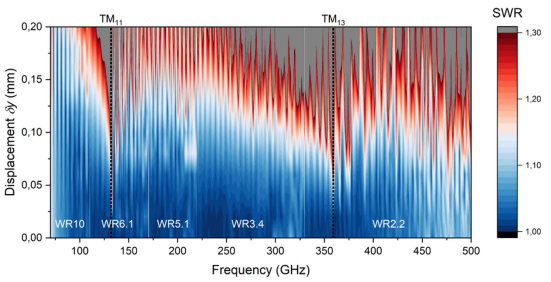

FIGURE 7. Standing wave ratio for an *E*-plane displacement. The influence of a symmetrical displacement, δy, on the standing wave ratio (SWR) was simulated using the electromagnetic model and illustrated as a contour plot. The standing wave pattern due to trapped TM_{11} and TM_{13} modes is evident. Note: Data is combined for each waveguide band WR-10, WR-6.5, WR-5.1, WR-3.4, and WR-2.2.

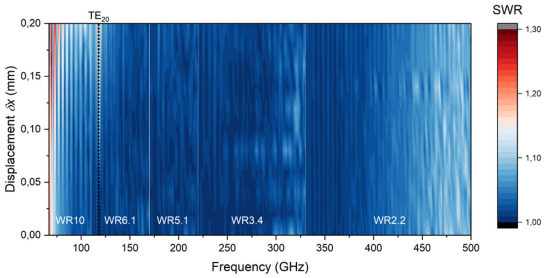

FIGURE 8. Standing wave ratio for an *H*-plane displacement. The influence of a symmetrical displacement, δx, on the standing wave ratio (SWR) was simulated using the electromagnetic model and illustrated as a contour plot. In this case, the onset of a TE_{20} mode is observed, but the standing wave ratio is almost immune to *H*-plane displacement. Note: Data is combined for each waveguide band WR-10, WR-6.5, WR-5.1, WR-3.4, and WR-2.2.

1100 GHz. On the other hand, the symmetrically displaced waveguide feed exhibits anomalies in the reflection coefficient associated with the onset of high-order mode propagation; see Fig. 6. In particular, the onset of a propagating TM_{11} mode at 132 GHz and a TM_{13} mode at 359 GHz are the primary causes of the observed degradation in the reflection coefficient for misaligned waveguide apertures. In contrast, other parasitic modes (Table 1) are less pronounced. The electromagnetic simulations were performed across all frequency bands for the aligned case (Fig. 5), whereas the frequency range of the misaligned case was restricted to below 500 GHz due to lack of *H*-plane symmetry and thereby substantial computational requirements (Fig. 6). Overall, the simulations and measurements show a good general agreement. The discrepancy can be attributed to the actual displacements (δx, δy) and to the fact that the EM model (mesh size) becomes very large with increasing frequency. For example, a 0.04-mm *E*-plane aperture misalignment between two WR-10 waveguides ($\delta y/b = 0.03$) causes a return loss of 40 dB[21], which roughly matches the accuracy of the "aligned" waveguides and explains the discrepancy between measurements and simulations of the ideally aligned case.

To acquire more insight, we calculated the standing wave ratio (SWR) from simulations of the reflection coefficient across a wide range of aperture misalignments. This mapping of the standing wave ratio condenses the data range and highlights overall behavior as well as the emergence of modes, illustrated by a contour plot against waveguide displacement and frequency. The simulations were conducted for both *E*-plane (Fig. 7) and *H*-plane (Fig. 8) displacements in increments of 0.02 mm. For the single-mode case (75–110 GHz), an increase in SWR is observed with increasing frequency for a symmetrical *E*-plane misalignment as expected for an equivalent shunt capacitor [20]. Conversely, the worst case is observed at low frequencies for a shunt inductive *H*-plane displacement [20]. The onset of propagating parasitic modes occurs at higher waveguide bands. For instance, the TE_{20} mode at 118 GHz is observed for an *H*-plane displacement. However, the results indicate a strong influence of the onset of the TM_{11} mode, as well as the higher TM_{13} mode. These modes will likely be coupled to an incident TE_{10} field at a misaligned *E*-plane junction. Additionally, the load absorbs the TM_{11} field less efficiently due to the E_x-field component. Therefore, the onset of a TM_{11} mode will cause ripples and degrade return loss; hence, the first TM mode is the primary concern when using an overmoded feed for a power sensor. Still, with careful alignment, $\delta y \leq 0.05$ mm, a return loss better than 20 dB is achieved (Fig. 7). In contrast, a misalignment in the *H*-plane has a minor impact on standing waves (Fig. 8) compared to *E*-plane displacement.

IV. CONCLUSION

A comprehensive study on the impact of symmetrically displaced waveguide feeds (aperture misalignments) on the return loss and standing waves of the PM5B power meter operating between 75 GHz and 1100 GHz has been presented. In cases with multiple possible propagating modes, the primary concerns are the onset of the TM_{11} mode at 132 GHz and the TM_{13} mode at 359 GHz. This occurs due to an *E*-plane displacement and is problematic for misalignments larger than $\delta y/b > 4\%$. The influence of *H*-plane displacements on return loss was found to be of minimal importance. In conclusion, properly aligning the waveguide apertures along the *E*-plane can effectively suppress the critical TM mode. These findings demonstrate that accurate power measurements across a wide frequency range, particularly for D-band (WR-6.5) applications, are feasible provided that the waveguides are aligned and fabricated with high tolerances.

ACKNOWLEDGMENT

The authors thank Patrik Blomberg and Shufei Sun for valuable feedback on the manuscript, Aditya Goturu and Divya Jayasankar for help with figures and LaTeX. Our co-author, Jeffrey Hesler, passed away on October 18th, 2025, surrounded by his family. He leaves a huge void, but we feel thankful to have known Jeffrey as a friend and to have had the opportunity to work with him. We will always cherish his memory and warmly dedicate this publication to honour him.

REFERENCES

[1] P. H. Siegel, "Terahertz technology," *IEEE Trans. Microw. Theory Techn.*, vol. 50, no. 3, pp. 910–928, Mar. 2002, doi: 10.1109/22.989974.

[2] Z. Popovic and E. N. Grossman, "THz metrology and instrumentation," *IEEE Trans. THz Sci. Technol.*, vol. 1, no. 1, pp. 133–144, Sep. 2011, doi: 10.1109/tthz.2011.2159553.

[3] R. A. Lewis, "A review of terahertz detectors," *J. Phys. D: Appl. Phys.*, vol. 52, no. 43, Aug. 2019, Art. no. 433001, doi: 10.1088/1361-6463/ab31d5.

[4] W. Herschel, "XIV. Experiments on the refrangibility of the invisible rays of the sun," *Philos. Trans. Roy. Soc. London*, vol. 90, pp. 284–292, Dec. 1800, doi: 10.1098/rstl.1800.0015.

[5] E. du Châtelet, "Dissertation sur la nature et la propagation du feu," Prault fils, Paris, 1744.

[6] A. C. Macpherson and D. M. Kerns, "A microwave microcalorimeter," *Rev. Sci. Instrum.*, vol. 26, pp. 27–33, Jan. 1955, doi: 10.1063/1.1771234.

[7] B. Vowinkel, "Broad-band calorimeter for precision measurement of millimeter- and submillimeter-wave power," *IEEE Trans. Instrum. Meas.*, vol. IM-29, no. 3, pp. 183–189, Sep. 1980, doi: 10.1109/tim.1980.4314903.

[8] N. Erickson, "A fast and sensitive submillimeter waveguide power meter," in *Proc. 10th Int. Symp. Space THz Technol.*, 1999, pp. 501–507.

[9] N. Erickson, "A fast, very sensitive calorimetric power meter for millimeter to submillimeter wavelengths," in *Proc. 13th Int. Symp. Space THz Technol.*, 2002, pp. 301–307.

[10] Virginia diodes, Inc., "VDI – Erickson Power Meters (PM5B)," Accessed: Dec. 18, 2025. [Online]. Available: https://vadiodes.com/vdi-erickson-power-meters-pm5/

[11] M. Celep et al., "Interlaboratory comparison of power measurements at millimetre- and sub-millimetre-wave frequencies," *Metrology*, vol. 4, no. 2, pp. 279–294, 2024, doi: 10.3390/metrology4020017.

[12] W. K. Perangin-Angin, K. Kuhlmann, and J. Rühaak, "Generalized efficiency and the uncertainty of millimeter wave power standard," *Adv. Radio Sci.*, vol. 21, pp. 7–13, 2023, doi: 10.5194/ars-21-7-2023.

[13] D. Stokes, Y. Liu, X. Shang, and N. M. Ridler, "Millimeter-wave and terahertz power meter characterisation at W-band frequencies," *J. Infrared, Millimeter, THz Waves*, vol. 44, pp. 134–150, Jan. 2023, doi: 10.1007/s10762-022-00898-8.

[14] M. Kinoshita, T. Inoue, K. Shimaoka, and K. Fujii, "Precise power measurement with a single-mode waveguide calorimeter in the 220–330 GHz frequency range," *IEEE Trans. Instrum. Meas.*, vol. 67, no. 6, pp. 1451–1460, Jun. 2018, doi: 10.1109/tim.2018.2795878.

[15] R. Johnson, "Design of linear double tapers in rectangular waveguides," *IEEE Trans. Microw. Theory Techn.*, vol. 7, pp. 374–378, Jul. 1959, doi: 10.1109/tmtt.1959.1124594.

[16] *IEEE Standard for Rectangular Metallic Waveguides and Their Interfaces for Frequencies of 110 GHz and Above–Part 1, Frequency Bands and Waveguide Dimensions*, IEEE Standard, 1785.1-2012, pp. 1–22, Mar. 2013, doi: 10.1109/IEEESTD.2013.6471987.

[17] *IEEE Standard for Rectangular Metallic Waveguides and Their Interfaces for Frequencies of 110 GHz and Above—Part 2: Waveguide Interfaces*, IEEE Standard 1785.2-2016, pp. 1–22, Sep. 2016, doi: 10.1109/IEEESTD.2016.7564020.

[18] D. F. Williams, "500 GHz–750 GHz rectangular-waveguide vector-network-analyzer calibrations," *IEEE Trans. THz Sci. Technol.*, vol. 1, no. 2, pp. 364–377, Nov. 2011, doi: 10.1109/tthz.2011.2127370.

[19] N. Marcuvitz, *Waveguide Handbook*. New York, NY, USA: McGraw-Hill, 1951.

[20] D. J. Bannister, E. J. Griffin, and T. E. Hodgetts, "On the dimensional tolerances of rectangular waveguide for reflectometry at millimetric wavelengths," Nat. Phys. Lab., Teddington, U.K., NPL Rep. DES 95, Sep. 1989.

[21] J. Hunter, "The displaced rectangular waveguide junction and its use as an adjustable reference reflection," *IEEE Trans. Microw. Theory Techn.*, vol. MTT-32, no. 4, pp. 387–394, Apr. 1984, doi: 10.1109/TMTT.1984.1132687.

[22] A. Wexler, "Solution of waveguide discontinuities by modal analysis," *IEEE Trans. Microw. Theory Techn.*, vol. MTT-15, no. 9, pp. 508–517, Sep. 1967, doi: 10.1109/TMTT.1967.1126521.

[23] H. Li, A. Arsenovic, J. L. Hesler, A. R. Kerr, and R. M. Weikle, "Repeatability and mismatch of waveguide flanges in the 500–750 GHz band," *IEEE Trans. THz Sci. Technol.*, vol. 4, pp. 39–48, Jan. 2014, doi: 10.1109/tthz.2013.2283540.

[24] M. Brady, "Cutoff wavelengths and frequencies of standard rectangular waveguides," *Electron. Lett.*, vol. 5, pp. 410–412, Aug. 1969, doi: 10.1049/el:19690310.

JAN STAKE (Fellow, IEEE) was born in Uddevalla, Sweden, in 1971. He received the M.Sc. degree in electrical engineering and the Ph.D. degree in microwave electronics from the Chalmers University of Technology, Gothenburg, Sweden, in 1994 and 1999, respectively.

In 1997, he was a Research Assistant with the University of Virginia, Charlottesville, VA, USA. From 1999 to 2001, he was a Research Fellow with the Millimetre Wave Group, Rutherford Appleton Laboratory, Didcot, U.K. He was a Senior RF/Microwave Engineer with Saab Combitech Systems AB, Gothenburg, Sweden, till 2003. From 2000 to 2006, he held various academic positions with the Chalmers University of Technology and from 2003 to 2006, he was the Head of the Nanofabrication Laboratory, Department of Microtechnology and Nanoscience (MC2). In 2006, he was appointed Professor and Head of the Terahertz and Millimetre Wave Laboratory, Chalmers University of Technology. He was a Visiting Professor with Submillimeter Wave Advanced Technology Group, Caltech/JPL, Pasadena, CA, USA, in 2007 and also with TU Delft, Delft, the Netherlands, in 2020. He received an appointment as a Visiting Research Fellow with the National Physical Laboratory, U.K., in 2023. He was the Co-Founder of Wasa Millimeter Wave AB, Gothenburg, Sweden. His research interests include high-frequency semiconductor devices, terahertz electronics, submillimeter wave measurement techniques, and terahertz systems.

Prof. Stake served as Editor-in-Chief of IEEE TRANSACTIONS ON TERAHERTZ SCIENCE AND TECHNOLOGY from 2016 to 2018 and Topical Editor from 2012 to 2015. From 2019 to 2021, he was the Chair of the IEEE THz Science and Technology Best Paper Award committee. He was an Elected Member of the International Society of Infrared, Millimeter and Terahertz Waves (IRMMW-THz) board between 2017 and 2024.

STEVEN DURANT received the B.S. and M.S. degrees in electrical engineering from the University of Virginia, Charlottesville, VA, USA, in 2010. He joined Virginia Diodes Inc., Charlottesville, VA, USA, developing custom terahertz systems and VNA extenders. His research interests include Schottky barrier diode mixer design, filter design, and VNA metrology.

LUCY WILLIAMSON graduated from the College of Charleston Charleston, South Carolina, in 2020. She received the B.S. degree in astrophysics and physics.

Her undergraduate research portfolio is diverse, including projects studying the evolution of novae, modeling exoplanet transit light curves, and the effect of episodic stellar activity on planet formation and evolution. From 2021 to 2022, she was a Research Scientist with Planetary Science Institute and collected infrared observations to map water in the nearby asteroid belt. This project segued into contracting for NASA Johnson Space Center, where she spent six months modeling asteroid data. In 2022, she was invited to speak with the Division of Planetary Sciences Conference, Ontario, to present the newly calibrated data analyzed while with NASA JSC. Since 2023, she has been a millimeter-wave engineer with Virginia Diodes, Charlottesville, VA, USA.

JEFFREY HESLER (Fellow, IEEE) received the B.S.E.E. degree from Virginia Tech, Blacksburg, VA, USA, in 1989, and the M.S.E.E. and Ph.D. degrees from the University of Virginia, Charlottesville, VA, USA, in 1991 and 1996, respectively. He became an Adjunct Professor with the Terahertz and Millimetre Wave Laboratory, Department of Microtechnology and Nanoscience (MC2), Chalmers University of Technology, Gothenburg, Sweden, in 2024. He was the President and Chief Technology Officer of Virginia Diodes Inc., Charlottesville and Visiting Research Assistant Professor with the University of Virginia. He has authored and coauthored more than 150 technical papers in refereed international conferences and journals, given talks at THz-focused workshops and conferences, such as IMS and EuMW. THz systems based on his innovative designs are now used in hundreds of research laboratories throughout the world. His research focuses on the creation of new technologies that are making possible the full exploitation of the Terahertz (THz) frequency band for scientific, defence, and industrial applications. He is a member of IEEE TC MTT-4 on THz Technology and Applications and serves as a reviewer for a variety of IEEE and IEE journals.